

Base Station Antenna Uptilt Optimization for Cellular-Connected Drone Corridors

Sung Joon Maeng, Md Moin Uddin Chowdhury, İsmail Güvenç, Arupjyoti Bhuyan, and Huaiyu Dai

Abstract—The concept of drone corridors is recently getting more attention to enable connected, safe, and secure flight zones in the national airspace. To support beyond visual line of sight (BVLOS) operations of aerial vehicles in a drone corridor, cellular base stations (BSs) serve as a convenient infrastructure, since such BSs are widely deployed to provide seamless wireless coverage. However, antennas in the existing cellular networks are down-tilted to optimally serve their ground users, which results in coverage holes if they are also used to serve drones. In this letter, we consider the use of additional uptilted antennas at cellular BSs and optimize the uptilt angle to minimize outage probability for a given drone corridor. Our numerical results show how the beamwidth and the maximum drone corridor height affect the optimal value of the antenna uptilt angle.

Index Terms—Antenna uptilt, drone corridor, national airspace (NAS), outage probability, UAV, UTM.

I. INTRODUCTION

Drones, also known as an unmanned aerial vehicles (UAVs), are rapidly gaining attention due to a wide range of promising applications. Commonly referred drone applications include search and rescue for public safety, commercial delivery service, and surveillance, among others [1]. According to the Federal Aviation Administration (FAA) forecast, the number of active UAVs is expected to reach 2 to 3 million by 2023 [2]. The framework for UAV traffic management (UTM) in the airspace has recently been developed by the FAA and the National Aeronautics and Space Administration (NASA) [3]. In this context, the concept of drone corridors has been gaining more attention, which serve as sky lanes that the UAVs are required to pass through for safe and secure flow of UAV traffic [4].

In cellular wireless networks, studies of drone applications typically fall under two categories: 1) base station mounted UAVs (UAV-BSs) that serve other ground and aerial users [5], [6], and 2) cellular connected UAVs (C-UAVs) that are users from the perspective of ground BSs [7], [8]. The success of future C-UAV operations (and in some cases, UAV-BS operations) relies critically on beyond visual line of sight (BVLOS) connectivity in drone corridors [3]. For example, the United Nations Children’s Fund (UNICEF) launched a drone testing corridor that monitors natural disasters, provides Wi-Fi signals, and delivers medical supplies for humanitarian purposes [9]. In addition, the drone taxi service operating in

aerial corridors has been tested by several companies. The optimal placement of the BSs and the number of antennas to support the drone corridor is studied in [10].

While cellular networks may provide reliable and seamless BVLOS connectivity to drones, the cellular BS antennas are optimized and down-tilted to best serve their ground users. As a result, this antenna setup is not appropriate to serve the drone corridor in the airspace. In this letter, we consider an additional set of uptilted cellular BS antennas to serve drones, and explore the optimal uptilt angles in order to provide a reliable coverage at a drone corridor. As a first work in this research direction, we design the drone corridor in a 2D coordinate system and consider two adjacent BSs, positioned across the drone corridor, to take into account the effect of the interference signal from the neighboring BS. Extending the study to 3D drone corridor design will be considered in future work. The contributions of our work can be summarized as follows: 1) We identify five unique cases for aerial coverage that are dependent on the uptilt angles and beamwidths of the ground BS antennas; 2) We derive closed-form expressions for the signal-to-interference plus noise ratio (SINR) outage probability and the average SINR over a drone corridor; 3) We find the optimal antenna uptilt angle that minimizes the SINR outage probability; 4) We show that the average SINR is maximized for an uptilt antenna angle in case 5 (see Fig. 1); 5) We show the effect of the beamwidth and the maximum drone corridor height on the SINR outage probability.

II. SYSTEM MODEL

We consider a 2D coordinate system for simplicity where the drone corridor is covered by two base stations (BS) as shown in Fig. 1. The horizontal distance between the two BSs is d_1 , and the lowest and the highest altitudes of the drone corridor are h_1 and h_2 , respectively. The BSs are equipped with a vertically directional antenna. The center angle of the directional beam is controlled by the uptilt angle α and the beamwidth of the antenna pattern is given by β . The height of the BSs is assumed to 0 [m] without loss of generality.

A. Probability Density Functions of the Location of UAVs

We assume that C-UAVs are uniformly distributed in the drone corridor area and served by the nearest BS. Then, the probability density function (PDF) of the horizontal (d_x) and vertical distance (h_x) of the UAVs to their serving BSs are given by

$$f_{d_x}(d_x) = \frac{2}{d_1}, [0 < d_x < d_1/2], \quad (1)$$

$$f_{h_x}(h_x) = \frac{1}{h_2 - h_1}, [h_1 < h_x < h_2]. \quad (2)$$

This work is supported in part by the INL Laboratory Directed Research Development (LDRD) Program under DOE Idaho Operations Office Contract DEAC07-05ID14517.

S. J. Maeng, M.M.U. Chowdhury, İ. Güvenç, and H. Dai are with the Department of Electrical and Computer Engineering, North Carolina State University, Raleigh, NC 27606 USA (e-mail: smaeng@ncsu.edu; mchowdh@ncsu.edu; iguven@ncsu.edu; hdai@ncsu.edu).

A. Bhuyan is with the INL Wireless Security Institute, Idaho National Laboratory, Idaho Falls, ID 83402 USA (e-mail: arupjyoti.bhuyan@inl.gov).

The elevation angles from the serving BS and the neighboring BS can be expressed as

$$\theta_1 = \tan^{-1}\left(\frac{h_x}{d_x}\right), \quad \theta_2 = \tan^{-1}\left(\frac{h_x}{d_1 - d_x}\right). \quad (3)$$

Then, the PDF of random variable θ_1 given h_x can be derived by the PDF transformation function as

$$\begin{aligned} f_{\theta_1}(\theta_1|h_x) &\stackrel{(a)}{=} \sum_{\theta_1=\tan^{-1}\left(\frac{h_x}{d_x}\right)} f_{d_x}\left(\frac{h_x}{\tan\theta_1}\right) \left|\frac{\partial d_x}{\partial \theta_1}\right| \\ &\stackrel{(b)}{=} f_{d_x}\left(\frac{h_x}{\tan\theta_1}\right) |h_x \cot^2\theta_1 + h_x| \\ &= \frac{2h_x}{d_1} \csc^2\theta_1, \left[\tan^{-1}\left(\frac{2h_x}{d_1}\right) < \theta_1 < \frac{\pi}{2}\right], \end{aligned} \quad (4)$$

where (a) comes from $d_x = \frac{h_x}{\tan\theta_1}$ and (b) comes from the fact that there is only one d_x satisfying $\theta_1 = \tan^{-1}\left(\frac{h_x}{d_x}\right)$.

B. Rectangular Beam pattern Model

We adopt the rectangular shape beam model for the directional antenna pattern, which is given by [11], [12]

$$g_y(\theta_y) = \begin{cases} G & \text{if } \alpha < \theta_y < \alpha + \beta \\ 0 & \text{otherwise} \end{cases}, \quad (5)$$

$$\alpha > 0, \quad \alpha + \beta < \frac{\pi}{2}, \quad (6)$$

where $g_y(\theta_y)$ and G denote the antenna pattern of the BS and the maximum antenna gain, respectively, and (6) indicates that the main beam is not steered downward and does not go beyond 90 degrees. In addition, $y \in \{1, 2\}$, and $y = 1, y = 2$ indicate the serving BS and the neighboring BS, respectively. We assume that the two BSs use the same uptilt angle (α) and beamwidth β . This model is simple but mathematically tractable and reflects adequately the effect of the directional beams.

C. Case Study for Increasing Uptilt Angle

We divide the drone corridor area into three regions depending on which beams cover portions of the drone corridor. As shown in Fig. 1, the area served only by the green or red beam of the serving BS is the ‘beam served region without interference’ (S), and the overlapping area of two beams is the ‘interference region’ (I), and the rest area (including that in the beam of the neighboring BS) is the ‘beam outage region’ (O). The illustrations of case 1 to case 5 show how the three areas change as the uptilt angle α increases. We found that it is necessary to analyze the performance case by case depending on the value of the uptilt angle. For example, the drone corridor area can be divided into the ‘beam outage region’ (O) and the ‘interference region’ (I) in case 1, while the ‘beam served region without interference’ (S) appears from h_1 to h_4 in case 2. Then, the ‘beam outage region’ (O) on cell edge area appears from h_1 to h_3 in case 3. As shown in Fig. 1c, we denote the heights of the crossing points of the beams from the two BSs as h_3 (center) and h_4 (side), given by:

$$h_3 = \frac{d_1}{2} \tan(\alpha), \quad h_4 = \frac{d_1}{\cot(\alpha) + \cot(\alpha + \beta)}. \quad (7)$$

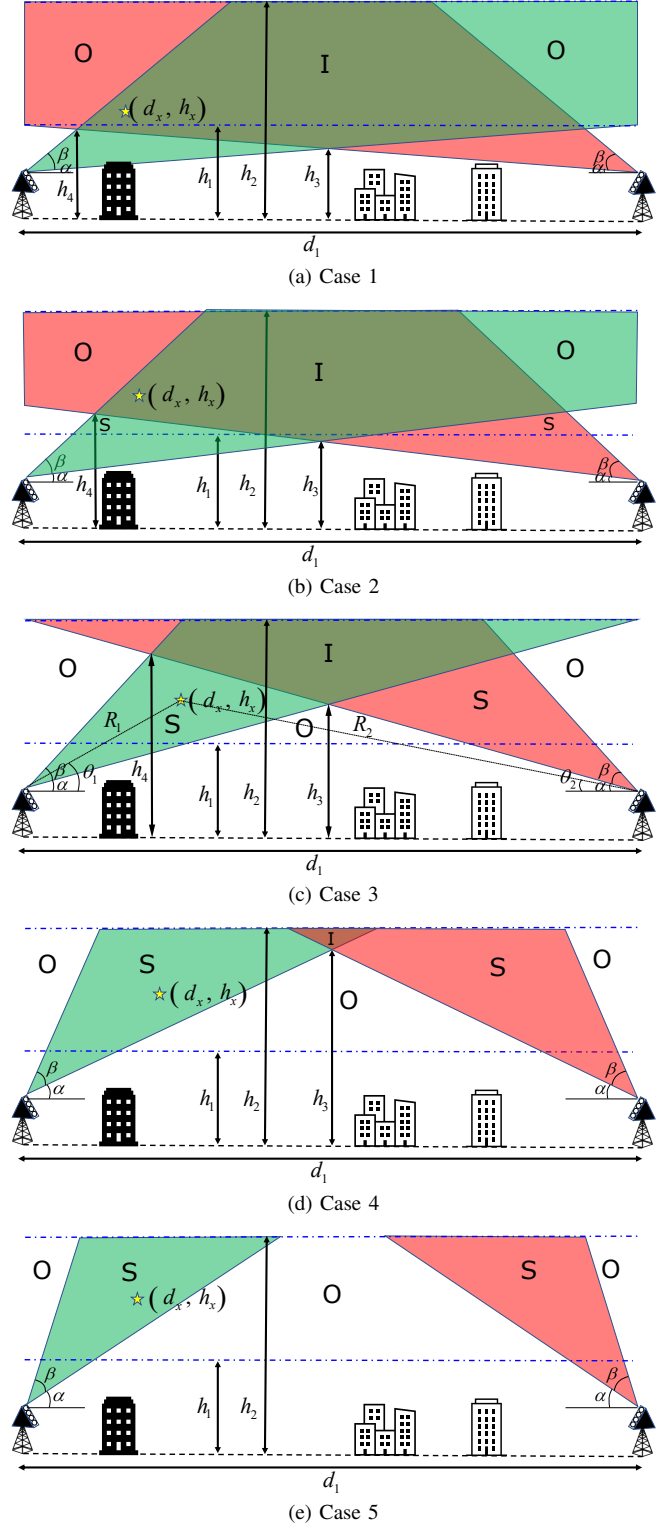


Fig. 1. The 2D coordinate drone corridor bounded by h_1 and h_2 , and the five different corridor coverage scenarios as the uptilt angle α grows.

The 3D distances between a UAV and the serving BS are denoted by R_1 , while the distance between a UAV and the neighboring BS is given by R_2 :

$$R_1 = \frac{h_x}{\sin(\theta_1)}, \quad R_2 = \frac{h_x}{\sin(\theta_2)}. \quad (8)$$

We consider free-space pathloss model, which is expressed as $PL = \left(\frac{4\pi R_1}{\lambda}\right)^2$. Then, signal-to-interference-plus-noise ratio

(SINR) can be written as

$$\text{SINR} = \frac{kg_1(\theta_1)/(R_1)^2}{kg_2(\theta_2)/(R_2)^2 + N_0}, \quad k = \frac{P_{\text{T}_x}\lambda^2}{16\pi^2}, \quad (9)$$

where P_{T_x} , λ , N_0 denote transmit power, wave-length, and noise power respectively, and $g_1(\theta_1)$, $g_2(\theta_2)$ indicate antenna gain of the serving and the neighboring BSs.

III. SINR OUTAGE PROBABILITY ANALYSIS

In this section, we derive the closed-form expression of SINR outage probability as a function of the uptilt angle (α). We can find the optimal uptilt angle that minimizes the outage probability from the obtained results. The SINR outage probability can be defined as follows

$$\text{Pr}_{\text{out}} = 1 - \text{Pr}_{\text{in}} = \text{Pr}(\text{SINR} < \tau), \quad (10)$$

where τ is the SINR threshold. We derive the SINR outage probability by obtaining the probability that a UAV is located at the beam outage region. Since the analytical expression can be different depending on the uptilt angle as shown in Fig. 1, we derive the analytical expressions separately considering three distinct cases. Note that we combine Case 1 and Case 2, and Case 3 and Case 4 as a two distinct cases.

A. Case 1 & 2 ($h_1 > h_3$)

In case 1 (Fig. 1a) and 2 (Fig. 1b), the green and red beams covers cell-edge drones ($d_x = \frac{d_1}{2}$) for all heights from h_1 to h_2 . In these cases, the beam served region with or without interference starts from the UAV at the center ($d_x = \frac{d_1}{2}$, $\theta_1 = \tan^{-1}\left(\frac{2h_x}{d_1}\right)$) and ends to the UAV at the left main beam edge ($\theta_1 = \alpha + \beta$) for all heights. We assume that the threshold level of SINR (τ) is designed to a moderate level, so that UAVs in the interference region are satisfied with SINR criteria. The probability that a UAV is located at the beam served region can be expressed as

$$\begin{aligned} \text{Pr}_{\text{in}} &= \int_{h_1}^{h_2} \int_{\tan^{-1}\left(\frac{2h_x}{d_1}\right)}^{\alpha+\beta} f_{\theta_1}(\theta_1|h_x)f_{h_x}(h_x)\partial\theta_1\partial h_x \\ &= \frac{-(h_1 + h_2)}{d_1} \cot(\alpha + \beta) + 1. \end{aligned} \quad (11)$$

Then, SINR outage probability can be written as

$$\text{Pr}_{\text{out}} = 1 - \text{Pr}_{\text{in}} = \frac{(h_1 + h_2)}{d_1} \cot(\alpha + \beta). \quad (12)$$

We can also obtain the first-order partial derivative with respect to α as follows

$$\frac{\partial \text{Pr}_{\text{out}}(\alpha)}{\partial \alpha} = \frac{-(h_1 + h_2)}{d_1} \csc^2(\alpha + \beta). \quad (13)$$

B. Case 3 & 4 ($h_1 < h_3 < h_2$)

In case 3 and 4, the elevation angle range of the beam served region can be divided into two parts; from h_1 to h_3 and from h_3 to h_2 . The SINR outage probability can be expressed as

$$\begin{aligned} \text{Pr}_{\text{out}} &= 1 - \int_{h_1}^{h_3} \int_{\alpha}^{\alpha+\beta} f_{\theta_1}(\theta_1|h_x)f_{h_x}(h_x)\partial\theta_1\partial h_x \\ &\quad - \int_{h_3}^{h_2} \int_{\tan^{-1}\left(\frac{2h_x}{d_1}\right)}^{\alpha+\beta} f_{\theta_1}(\theta_1|h_x)f_{h_x}(h_x)\partial\theta_1\partial h_x \\ &= 1 + \frac{(h_1 + h_2)}{d_1} \cot(\alpha + \beta) \\ &\quad - \frac{d_1^2 \tan^2(\alpha) - h_1^2}{d_1(h_2 - h_1)} \cot(\alpha) - \frac{h_2 - \frac{d_1}{2} \tan(\alpha)}{h_2 - h_1}. \end{aligned} \quad (14)$$

We can also obtain the first-order partial derivative with respect to α as follows

$$\begin{aligned} \frac{\partial \text{Pr}_{\text{out}}(\alpha)}{\partial \alpha} &= -\frac{(h_1 + h_2)}{d_1} \csc^2(\alpha + \beta) \\ &\quad + \frac{d_1}{4(h_2 - h_1)} \sec^2(\alpha) - \frac{(h_1)^2}{d_1(h_2 - h_1)} \csc^2(\alpha). \end{aligned} \quad (15)$$

C. Case 5 ($h_3 > h_2$)

In case 5, the elevation angle range of the beam served area is from α to $\alpha + \beta$ for all heights. The SINR outage probability can be written as

$$\begin{aligned} \text{Pr}_{\text{out}} &= 1 - \int_{h_1}^{h_2} \int_{\alpha}^{\alpha+\beta} f_{\theta_1}(\theta_1|h_x)f_{h_x}(h_x)\partial\theta_1\partial h_x \\ &= 1 + \frac{(h_1 + h_2)}{d_1} (\cot(\alpha + \beta) - \cot(\alpha)). \end{aligned} \quad (16)$$

The first-order partial derivative is given by

$$\frac{\partial \text{Pr}_{\text{out}}(\alpha)}{\partial \alpha} = -\frac{(h_1 + h_2)}{d_1} (\csc^2(\alpha + \beta) - \csc^2(\alpha)). \quad (17)$$

Now that we obtain the SINR outage probability (Pr_{out}) and the first-order partial derivative, we can find the optimal uptilt angle (α) by using an optimization method like gradient descent if the function is convex.

IV. AVERAGE SINR ANALYSIS

In this section, we calculate the average SINR of UAVs in the drone corridor. We separately derive the expressions depending on the cases in Fig. 1 as the uptilt angle increases. From (9), the definition of the average SINR of drones in the whole drone corridor area is given by

$$\begin{aligned} \text{SINR}_{\text{avg}} &= \mathbb{E}[\text{SINR}] \\ &= \int_{h_1}^{h_2} \int_{\tan^{-1}\left(\frac{2h_x}{d_1}\right)}^{\frac{\pi}{2}} \left(\frac{kg_1(\theta_1)/(R_1)^2}{kg_2(\theta_2)/(R_2)^2 + N_0} \right) \\ &\quad \times f_{\theta_1}(\theta_1|h_x)f_{h_x}(h_x)\partial\theta_1\partial h_x. \end{aligned} \quad (18)$$

1) *Case 1* ($h_1 > h_3$ & $h_1 > h_4$): The whole beam served area is 'interference region' in case 1. The average SINR can be written as

$$\begin{aligned} \text{SINR}_{\text{avg}} &= \int_{h_1}^{h_2} \int_{\tan^{-1}\left(\frac{2h_x}{d_1}\right)}^{\alpha+\beta} \left(\frac{(R_2)^2}{(R_1)^2} \right) f_{\theta_1}(\theta_1|h_x)f_{h_x}(h_x)\partial\theta_1\partial h_x \\ &= \int_{h_1}^{h_2} \left(\frac{2d_1}{h_x(h_2 - h_1)} \right) \left(\alpha + \beta - \tan^{-1}\left(\frac{2h_x}{d_1}\right) \right) \end{aligned}$$

$$\begin{aligned}
& - \left(\frac{4}{h_2 - h_1} \right) \\
& \times \left(\log(\sin(\alpha + \beta)) - \log \left(\sin \left(\tan^{-1} \left(\frac{2h_x}{d_1} \right) \right) \right) \right) \\
& - \left(\frac{2h_x}{d_1(h_2 - h_1)} \right) \left(\cot(\alpha + \beta) - \frac{d_1}{2h_x} \right) \partial h_x. \quad (20)
\end{aligned}$$

Note that we assume the interference dominant condition so that we neglect the noise term. We neglect the ‘beam outage region’ where θ_1 is from $\alpha + \beta$ to $\frac{\pi}{2}$ in the calculation, since $\text{SINR} \approx 0$.

2) *Case 2* ($h_3 < h_1 < h_4$): From case 2 to case 5, we only consider ‘beam served region without interference’ (green region) since the average SINR is dominant by that region. Then, the average SINR can be expressed as

$$\begin{aligned}
\text{SINR}_{\text{avg}} &= \int_{h_1}^{h_4} \int_{\gamma}^{\alpha+\beta} \left(\frac{kG}{N_0(R_1)^2} \right) f_{\theta_1}(\theta_1|h_x) f_{h_x}(h_x) \partial \theta_1 \partial h_x \\
&= \int_{h_1}^{h_4} \left(\frac{2kG}{d_1 N_0 (h_2 - h_1) h_x} \right) \\
&\times \left(\alpha + \beta - \cot^{-1} \left(\frac{d_1}{h_x} - \cot(\alpha) \right) \right) \partial h_x, \quad (21)
\end{aligned}$$

where $\gamma = \cot^{-1} \left(\frac{d_1}{h_x} - \cot(\alpha) \right)$ indicates the elevation angle at the right end point of green region. We can derive γ as follow: the relation between θ_1 and θ_2 is written from (3) as

$$\cot(\theta_2) = \frac{d_1}{h_x} - \cot(\theta_1). \quad (22)$$

Then, we can obtain γ by plugging in $\theta_1 = \gamma$, $\theta_2 = \alpha$.

3) *Case 3* ($h_1 < h_3 < h_2$ & $h_2 > h_4$): The elevation angle range that we are concerned is different from h_1 to h_3 and from h_3 to h_4 . Then, the average SINR can be written as

$$\begin{aligned}
\text{SINR}_{\text{avg}} &= \int_{h_1}^{h_3} \int_{\alpha}^{\alpha+\beta} \left(\frac{kG}{N_0(R_1)^2} \right) f_{\theta_1}(\theta_1|h_x) f_{h_x}(h_x) \partial \theta_1 \partial h_x \\
&+ \int_{h_3}^{h_4} \int_{\gamma}^{\alpha+\beta} \left(\frac{kG}{N_0(R_1)^2} \right) f_{\theta_1}(\theta_1|h_x) f_{h_x}(h_x) \partial \theta_1 \partial h_x \\
&= \int_{h_1}^{h_3} \left(\frac{2kG\beta}{d_1 N_0 (h_2 - h_1) h_x} \right) \partial h_x + \int_{h_3}^{h_4} \left(\frac{2kG}{d_1 N_0 (h_2 - h_1) h_x} \right) \\
&\times \left(\alpha + \beta - \cot^{-1} \left(\frac{d_1}{h_x} - \cot(\alpha) \right) \right) \partial h_x. \quad (23)
\end{aligned}$$

4) *Case 4* ($h_1 < h_3 < h_2$ & $h_2 < h_4$): The average SINR can be written as

$$\begin{aligned}
\text{SINR}_{\text{avg}} &= \int_{h_1}^{h_3} \int_{\alpha}^{\alpha+\beta} \left(\frac{kG}{N_0(R_1)^2} \right) f_{\theta_1}(\theta_1|h_x) f_{h_x}(h_x) \partial \theta_1 \partial h_x \\
&+ \int_{h_3}^{h_2} \int_{\gamma}^{\alpha+\beta} \left(\frac{kG}{N_0(R_1)^2} \right) f_{\theta_1}(\theta_1|h_x) f_{h_x}(h_x) \partial \theta_1 \partial h_x \\
&= \int_{h_1}^{h_3} \left(\frac{2kG\beta}{d_1 N_0 (h_2 - h_1) h_x} \right) \partial h_x + \int_{h_3}^{h_2} \left(\frac{2kG}{d_1 N_0 (h_2 - h_1) h_x} \right) \\
&\left(\alpha + \beta - \cot^{-1} \left(\frac{d_1}{h_x} - \cot(\alpha) \right) \right) \partial h_x. \quad (24)
\end{aligned}$$

TABLE I
SIMULATION SETTINGS

Parameter	Value
Transmit power (P_{T_x})	30 dBm
Horizontal distance between BSs (d_1)	1000 m
Minimum drone corridor height (h_1)	100 m
Maximum drone corridor height (h_2)	[200, 300, 400, 500] m
Threshold level of SINR (τ)	-3 dB
Maximum antenna gain (G)	297.6/ β dB [13]
Carrier frequency	3 GHz
Bandwidth (BW)	100 MHz
Thermal noise (TN)	-174 dBm/Hz
Noise figure (NF)	9 dB

5) *Case 5* ($h_3 > h_2$): The average SINR can be written as

$$\begin{aligned}
\text{SINR}_{\text{avg}} &= \int_{h_1}^{h_2} \int_{\alpha}^{\alpha+\beta} \left(\frac{kG}{N_0(R_1)^2} \right) f_{\theta_1}(\theta_1|h_x) f_{h_x}(h_x) \partial \theta_1 \partial h_x \\
&= \int_{h_1}^{h_2} \left(\frac{2kG\beta}{d_1 N_0 (h_2 - h_1) h_x} \right) \partial h_x. \quad (25)
\end{aligned}$$

V. NUMERICAL RESULTS

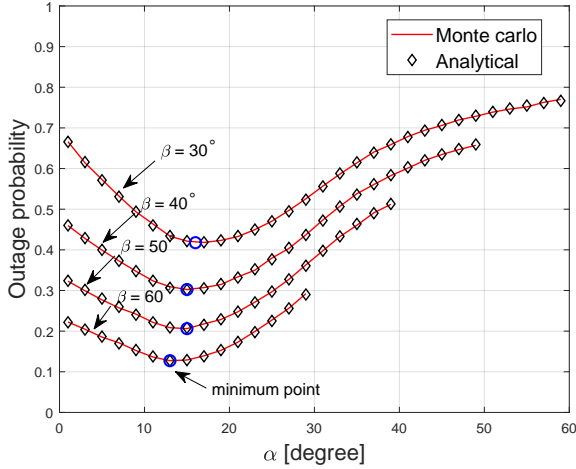
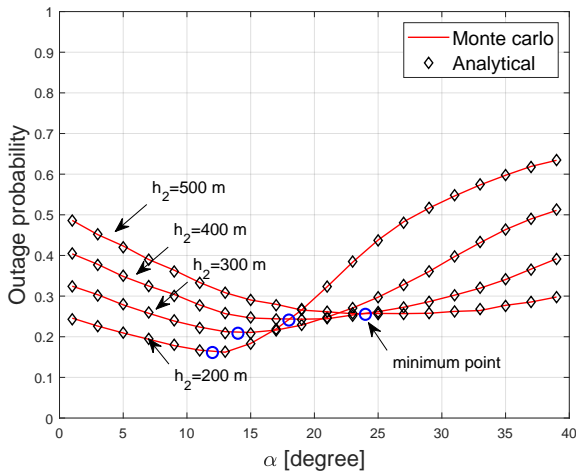
In this section, we present simulation results to verify above analysis and evaluate the performance depending on the up tilt angle. The key parameters are listed in Table I. In general, the maximum antenna gain (G) is inversely proportional to the beamwidth (β). In other words, as the beam becomes sharper, the maximum beam gain is higher. We adopt the result in [13, Table II] to calculate the antenna gain. Noise power is calculated by $N_0 = (\text{TN}) + 10 \log_{10}(\text{BW}) + (\text{NF})$ [dBm].

Fig. 2 shows the SINR outage probability with respect to the up tilt angle. We use (10) to obtain Monte Carlo results and use (12), (14), (16) to get analytical results. It is observed that the SINR outage probability is a convex function with respect to α , so that we can obtain the global minimum by the first-order partial derivative, and the optimal point that minimizes the outage probability is different depending on beamwidth (β) and the maximum drone corridor height (h_2). We also observe that the performance with the optimal up tilt angle (α) improves as the beamwidth increases and the maximum drone corridor height decreases.

In Fig. 3, it is shown that the average SINR increases as the up tilt angle grows and converges to the maximum value. The Monte Carlo results are obtained by (18) and the analytical results are obtained by (20)-(25). Intuitively, the best average SINR is achieved as Case 5 emerges, where the whole beamwidth (from $\theta_1 = \alpha$ to $\theta_1 = \alpha + \beta$) is inside of the drone corridor without interference for all heights from h_1 to h_2 . It is also observed that the maximum average SINR increases as beamwidth (β) and the maximum height of the drone corridor (h_2) decreases.

VI. CONCLUSION

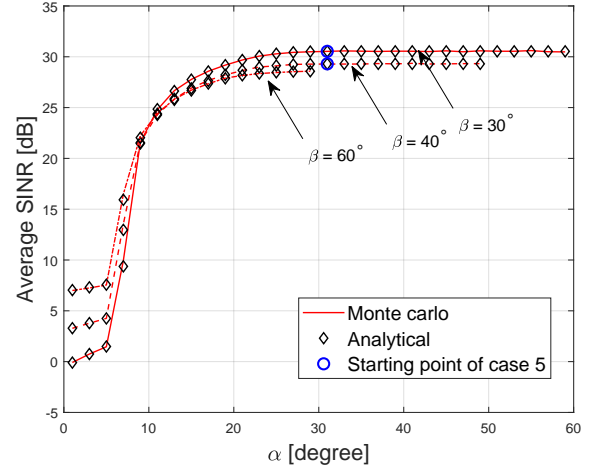
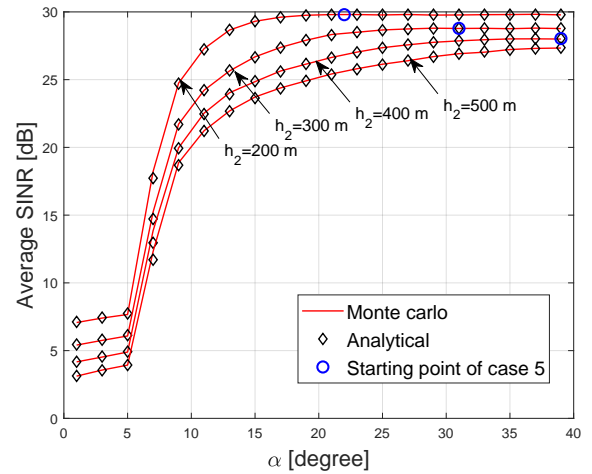
In this paper, we study the optimal up tilt angle of the antenna for cellular-connected drone corridor communication. We consider two BSs with 2D coordinates and the directional antenna pattern. We derive the closed-form expressions of SINR outage probability and average SINR to evaluate the performance. We found that the SINR outage probability is a convex function of the up tilt angle, and the average SINR is maximized from a certain degree of the up tilt angle which is

(a) SINR outage probability with $h_2 = 300$ m.(b) SINR outage probability with $\beta = 50^\circ$.Fig. 2. SINR outage probability depending on the uptilt angle (α).

the starting point of Case 5 in our five identified scenarios. Furthermore, it is shown that wide beamwidth is preferred in terms of the outage probability, while narrow beamwidth is desired from the perspective of the average SINR. A lower maximum height of the drone corridor will benefit both performance criteria. Although our study is limited to the 2D coordinate system, considering a scenario where the BSs are deployed along the drone corridor, our results and findings can be conveniently extended to 3D drone corridor design.

REFERENCES

- [1] V. Marojevic, I. Guvenc, R. Dutta, M. L. Sichitiu, and B. A. Floyd, "Advanced Wireless for Unmanned Aerial Systems: 5G Standardization, Research Challenges, and AERPAW Architecture," *IEEE Veh. Technol. Mag.*, vol. 15, no. 2, pp. 22–30, Apr. 2020.
- [2] Federal Aviation Administration (FAA). (2019) FAA Aerospace Forecast, Fiscal Years 2019-2039. [Online]. Available: www.faa.gov/data_research/aviation/aerospace_forecasts/media/FY2019-39_FAA_Aerospace_Forecast.pdf
- [3] Federal Aviation Administration (FAA). (2020) UTM Concept of Operations Version 2.0. [Online]. Available: https://www.faa.gov/uas/research_development/traffic_management/media/UTM_ConOps_v2.pdf
- [4] A. Bhuyan, I. Guvenc, H. Dai, M. L. Sichitiu, S. Singh, A. Rahmati, and S. J. Maeng, "Secure 5G network for a nationwide drone corridor," in *Proc. IEEE Aerospace Conf.*, 2021, pp. 1–10.

(a) Average SINR with $h_2 = 300$ m.(b) Average SINR with $\beta = 50^\circ$.Fig. 3. Average of SINR depending on the uptilt angle (α).

- [5] D. Xu, Y. Sun, D. W. K. Ng, and R. Schober, "Multiuser MISO UAV communications in uncertain environments with no-fly zones: Robust trajectory and resource allocation design," *IEEE Trans. Commun.*, vol. 68, no. 5, pp. 3153–3172, Jan. 2020.
- [6] Y. Yapıcı, N. Rupasinghe, I. Guvenc, H. Dai, and A. Bhuyan, "Physical layer security for NOMA transmission in mmWave drone networks," *IEEE Trans. Veh. Technol.*, vol. 70, no. 4, pp. 3568–3582, Mar. 2021.
- [7] W. Miao, C. Luo, G. Min, Y. Mi, and Z. Yu, "Location-based Robust Beamforming Design for Cellular-enabled UAV Communications," *IEEE Internet Things J.*, Oct. 2020.
- [8] C. D'Andrea, A. Garcia-Rodriguez, G. Geraci, L. G. Giordano, and S. Buzzi, "Analysis of UAV communications in cell-free massive MIMO systems," *IEEE Open J. Commun. Soc.*, vol. 1, pp. 133–147, Jan. 2020.
- [9] United Nations Children's Fund (UNICEF). (2017) Humanitarian drone corridor launched in Malawi. [Online]. Available: <https://www.unicef.org/stories/humanitarian-drone-corridor-launched-malawi>
- [10] S. Singh, U. Bhattacherjee, E. Öztürk, I. Guvenc, H. Dai, M. Sichitiu, and A. Bhuyan, "Placement of mmwave base stations for serving urban drone corridors," in *Proc. IEEE Veh. Technol. Conf. (VTC)*, Apr. 2021.
- [11] R. Kovalchukov, D. Moltchanov, A. Samuylov, A. Ometov, S. Andreev, Y. Koucheryav, and K. Samouylov, "Analyzing effects of directionality and random heights in drone-based mmWave communication," *IEEE Trans. Veh. Technol.*, vol. 67, no. 10, pp. 10064–10069, Jul 2018.
- [12] W. Yi, Y. Liu, E. Bodanese, A. Nallanathan, and G. K. Karagiannidis, "A unified spatial framework for UAV-aided mmWave networks," *IEEE Trans. Commun.*, vol. 67, no. 12, pp. 8801–8817, Oct. 2019.
- [13] K. Venugopal, M. C. Valenti, and R. W. Heath, "Device-to-device millimeter wave communications: Interference, coverage, rate, and finite topologies," *IEEE Trans. Wireless Commun.*, vol. 15, no. 9, pp. 6175–6188, Jun. 2016.